ACOUSTIC FIELD COHERENCE IN FOUR-DIMENSIONALLY VARIABLE SHALLOW WATER ENVIRONMENTS: ESTIMATION USING CO-LOCATED HORIZONTAL AND VERTICAL LINE ARRAYS

Timothy F. Duda[a], Jon M. Collis[b,a]

[a]Woods Hole Oceanographic Institution, Woods Hole, MA 02543 USA
[b]Boston University, Boston, MA 02215 USA

Tim Duda, Woods Hole Oceanographic Institution, MS #11, Woods Hole, MA 02543 USA, tduda@whoi.edu

Abstract: *The implementation of two- and three-dimensional acoustic receiver arrays is challenging in the ocean environment. Fixed geometry and connectivity can only be built and maintained at great expense. However, such ideal arrays can be very powerful for signal detection, classification, and tracking, although many of the signal-processing methods employed are subject to constraints of acoustic field temporal and spatial coherence. Thus, understanding the processes at work determining coherence is essential because system effectiveness may then be predictable from environmental parameter input. To study acoustic fields and coherence over finite aperture, the research community has recently taken steps to enable routine use of co-located horizontal and vertical line arrays, typically arranged in the shape of the Roman letter L (or Greek Γ), with the horizontal leg on the seafloor. This is a small subset of all possible geometries, but it enables measurements of acoustic field coherence not possible with single line arrays. Here, new L-array measurements made in the SW06 field program are used to measure coherence and test coherence predictions via joint analysis of vertical and horizontal line array receptions. Impulsive mode arrivals (including mode multipath) from fixed sources will be estimated using the vertical array. Signals on the horizontal array, which is neither broadside nor endfire, will be compared with signals synthesized using the mode arrivals to estimate azimuthal decorrelation effects. Results can be compared with coherence estimates from computational and theoretical studies.*

Keywords: *Shallow-water acoustics, receiver array, L-array, coherence, normal modes*

1. INTRODUCTION

Underwater acoustic measurement systems, specifically multi-dimensional receiver arrays designed for low and middle frequency sensing, can provide powerful signal gain and noise suppression under ideal conditions. However, gain can be compromised by short spatial and temporal coherence lengths [1,2]. Environmental processes and geometries determine these coherence scales. These processes can sometimes be treated with parameterizations, such as geoacoustic models or seafloor roughness parameters, but not always. Knowledge of the spatial and temporal coherencies is a requirement for optimizing signal processing schemes, and therefore so is knowledge of the processes at work and their parameterizations, if available.

One recent focus of research has been the effect that nonlinear internal wave packets can have on temporal and spatial coherence in shallow waters [3,4]. A useful tool for field validation of such studies is the unified horizontal and vertical line array [1]. Deployments of such arrays often have an L-configuration, with a vertical line array (VLA) rising from a bottom-mounted horizontal line array (HLA), have been used to identify and quantify the environmental factors influencing coherence length. They can also be used to collect data for bottom inversion [5]. The SW06 field program, which took place from late July to early September 2006 to the east of the New Jersey (USA) coast, made use of various source and receiver configurations, including a 48-element receiver array placed by WHOI [6]. The array was divided into two sections: a 16-element vertical line array spanning four-fifths of the water column (water depth 80 m) and a 32-element horizontal line array, 472 m in length. Specific source transmissions considered are low- to mid-frequency ranging from 101 to 1627 Hz, and run parallel to the continental shelf. To analyze coherence we introduce a procedure tailored to non-broadside incidence on the HLA. Mode interference that occurs over range will introduce signal variability along the HLA which we would like to separate from transverse signal decorrelation effects that might be introduced by azimuthally-varying propagation.

This paper presents preliminary SW06 observations and results. In Sec. 2, we discuss the experiment and the signal processing techniques. Coherence length is discussed, and related observations of specific acoustic arrivals are presented in Sec. 3. Section 4 gives a more detailed discussion of coherence length and Sec. 5 gives concluding remarks.

2. ACOUSTIC MEASUREMENT AND PROCESSING

The acoustic and oceanographic data discussed in this paper were collected during the Shallow-water shelf-break 2006 (SW06) experiment conducted off the coast of New Jersey. The SW06 experiment was a United States Office of Naval Research effort performed 100 miles east of New Jersey on the continental shelf at the shelf-break [6], lasting from mid-July to mid-September, 2006. Canadian investigators were also involved. A total of 62 acoustic and oceanographic moorings were deployed, all but a few by personnel from the Woods Hole Oceanographic Institution (WHOI), with the majority following a “T” shaped geometry. One leg had an along-shelf alignment following (approximately) the 80 m isobath, at heading 30°, the other was across-shelf from depths of 58 to 500 meters (heading 300°). A cluster of moorings was placed at the intersection of the two axes to create a densely populated volumetric measure of 3-dimensional physical oceanography, nonlinear internal wave packets in particular. This was also the

location of the WHOI L array (Fig. 1). Moored acoustic sources were placed near the far end of the along-shelf line, at approximately 20-km range, and along the inshore end of the cross-shelf line (the cap of the T), to provide known signals for monitoring propagation characteristics along the two paths.

Specific sound pulses considered in this paper were produced by the Miami Sound Machine source, located 19.75 km from the L-array at a heading of about 25 degrees. Figure 1 depicts the source and receiver geometry for the Miami Sound Machine (MSM) and L-array configuration used during SW06. Acoustic signals arrived first at the north end of the HLA and arrived last at the VLA. Once each half hour the source emitted a sequence of PN coded 100-Hz pulses (90 s, 36 pulses), then 200 Hz pulses, 400 Hz, 800 Hz and 1600 Hz. In this paper only one pulse from a given sequence will be examined.

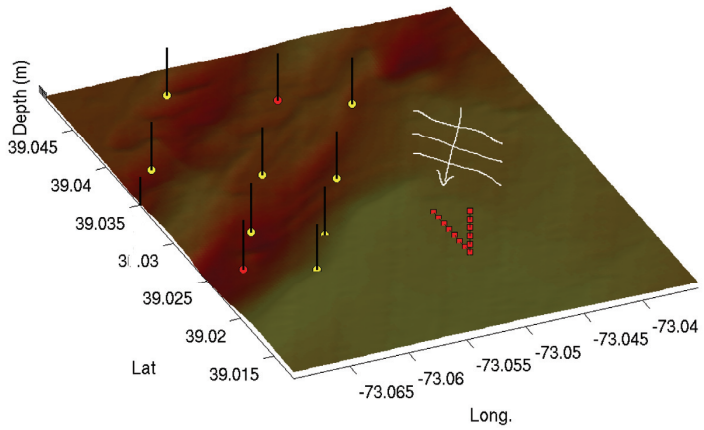

Fig.1: A depiction of MSM acoustic arrivals at the SW06 WHOI L array. The horizontal leg of the array is aligned very close to north/south. The bearing to the MSM sound source is 25.68 degrees at the south (VLA) end of the array.

Here, we introduce a very simple technique to evaluate acoustic field variability and coherence in planes transverse to the acoustic propagation direction. This variability can be measured directly only for signals with broadside incidence, otherwise something else needs to be done because of expected range variability of sound trapped in the shallow water waveguide. Explained simply, the VLA is used to obtain a normal mode description of the field at that point. The field at the HLA positions that would result from those modes is then computed. This has a degree of horizontal decorrelation not resulting from scattering processes. Comparison of this field with the measured field may provide useful information about azimuthal (transverse) field variability.

Explaining the procedure in more detail, first the acoustic arrivals on the horizontal and vertical line arrays are processed to obtain the time-synchronized complex acoustic pressure, $p(t,j)$, j = 1..48, at each element along the L-array. Using temperature data collected along the VLA to determine sound speed profiles, the normal mode functions and associated wavenumber values can be determined using a simplified geoacoustic model of the site [7]. Given the acoustic pressure along the VLA, mode filtering can be used to obtain time-series of mode content at the VLA. From this, a benchmark acoustic field along the HLA can be synthesized for comparison with the data. The acoustic signal along the VLA can be written as an N-term modal sum,

$$p(z,t) = \sum_{n=1}^{N} A_n(t)\phi_n(z,t) \tag{1}$$

where p is the complex pressure, A_n are the mode coefficients, and ϕ_n the vertical mode functions. The sampling of the pressure field is discretely limited in that it is only sampled at 16 hydrophone locations in the water column. For the 100-Hz arrivals fewer than 16 modes are expected to arrive, so the pseudoinverse (generalized inverse) method is suitable for obtaining the mode coefficients [8].

An adjustment of phase and use of the mode shape at the seafloor is all that is needed to construct the field at a bottom-resting HLA. For positions (Δx, Δy, z) where the x-direction is toward the source, the synthesized field is given by

$$p_s(z,t) = \sum_{n=1}^{N} A_n(t)\phi(z,t)e^{ik\Delta x}. \tag{2}$$

For a linear array and angle of incidence θ, $\Delta x = \Delta y / \tan\theta$, and distance along the array is given by $l = (\Delta x^2 + \Delta y^2)^{1/2}$. For a bottom resting HLA position, $z = z_{max}$. We refer to this synthesized modal field as the fixed-mode field. Comparing this with the measured field allows us to detect laterally variable (but adiabatic produced) mode amplitude and phase along the HLA, and/or the effects along the HLA of laterally variable mode coupling. Of course, low signal to noise ratio and incorrect mode shapes will give errors in $A_n(t)$ and p_s. We are investigating the effect of these on the results.

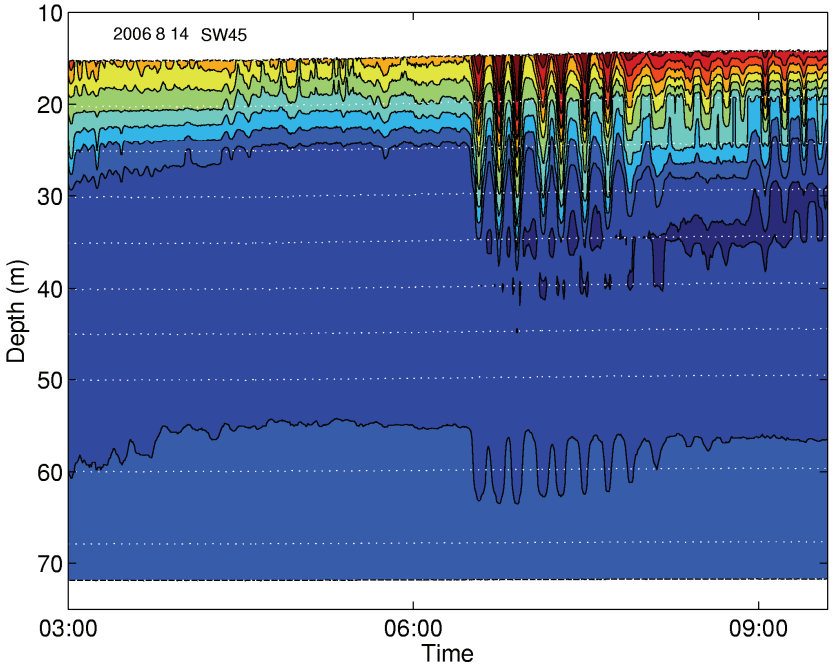

Fig.2: A contour plot of isotherms measured by a mooring near the acoustic source. The dotted lines show thermometer depths. Contour intervals are 1.5 °C.

3. MEASURED AND SYNTHETIC HLA AND VLA FIELDS

Here, two 100-Hz broadband pulses arriving at the array are analyzed. One is from a time with very small internal waves between the source and receiver, determined by sensors on moorings near the source, near the receiver, and approximately centred between them (Fig. 2, left). The other pulse is from a period when a packet of nonlinear waves was in the source-receiver path (Fig. 2, right).

Figure 3 shows the measured intensity time series, in dB, during a time of calm ocean state (Fig. 2, left). Modes one to four are dispersed fully and can be seen easily by eye. At the top, the A_n are shown. Below and to the right is the field synthesized using a four-term modal sum. Along the vertical array the match is very good. The synthetic and measured fields differ from each other along the horizontal array, specifically the higher-order, 3rd and 4th modes.

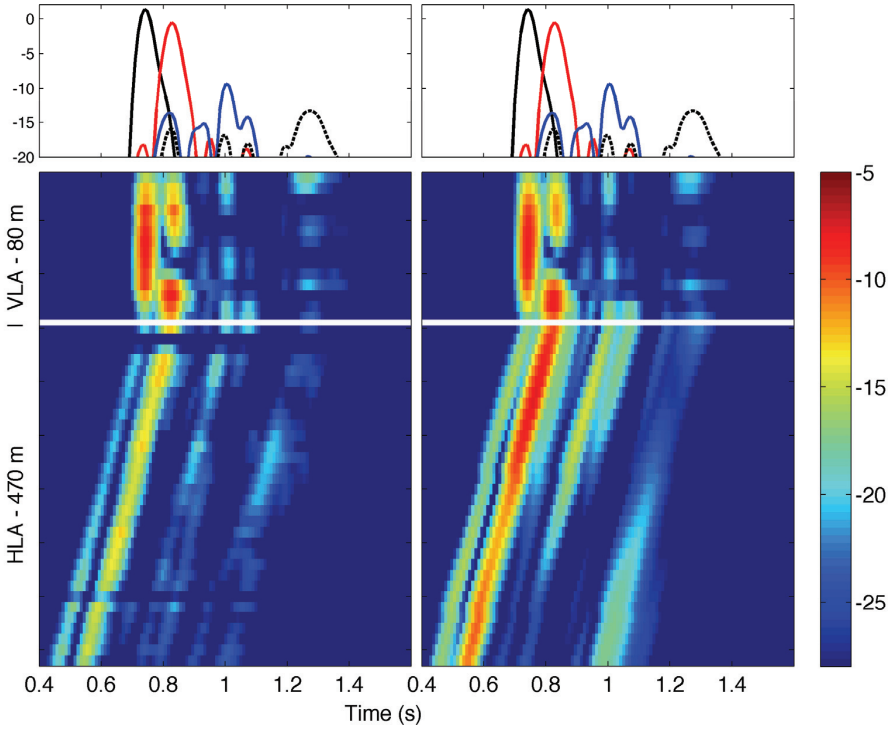

Fig.3: (left, lower) Intensity as a function of time along the L-array during a low-internal wave period. The signal arrived at the tip of the horizontal array first. (left, center) Intensity at the VLA is shown, with the deeper phones at the bottom. (left, top) The result of mode decomposition is shown: mode 1 (black), mode 2 (red), mode 3 (blue) and mode 4 (dash black). On the right, the mode content plot is repeated at the top, and the synthesized intensity, $10\log(p_s^2)$, at every VLA and HLA position is shown below. Note that the reference acoustic pressure for intensity calculations is arbitrary -- source reference calibrations have not been performed.

Figure 4 shows a measured and synthesized intensity time series during the strong internal wave period (Fig. 2, 06:30). There are multiple and extended arrivals of the modes along the L-array. The match between the measured and synthesized fields is again

very good along the vertical array, however the agreement along the horizontal array is poor, with all of the modes generally disagreeing.

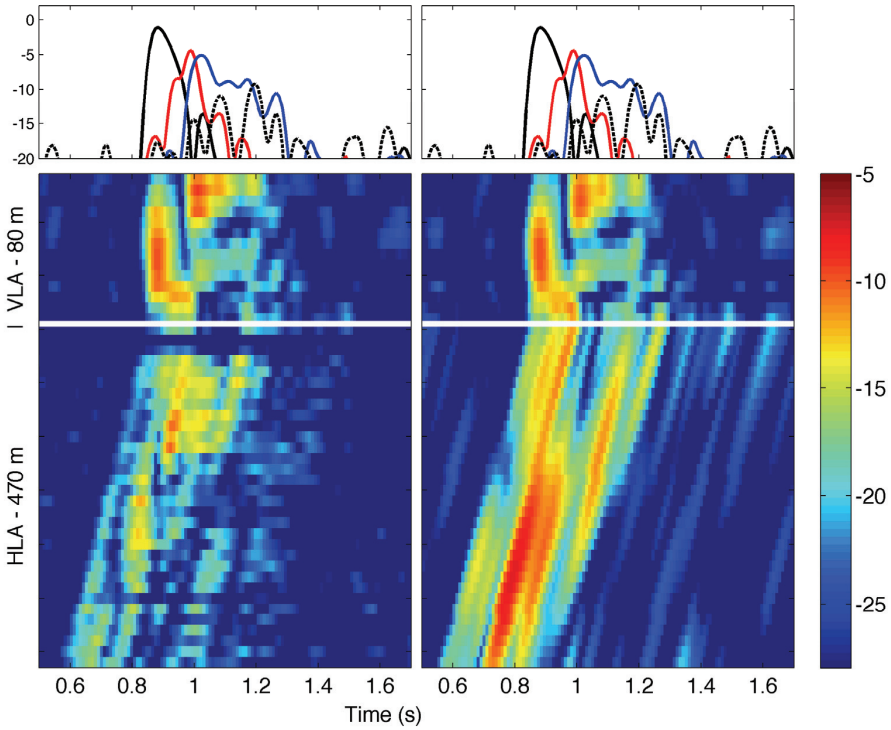

Fig.4: (left, lower) Intensity as a function of time along the L-array during the high-internal wave period. (left, center) Intensity at the VLA is shown. (left, top) The result of mode decomposition is shown: mode 1 (black), mode 2 (red), mode 3 (blue) and mode 4 (dash black). On the right, the synthesized intensity at every L-array position is shown. Note that the transmission shown is at 06:30 from Fig. 2.

4. COHERENCE ESTIMATES

Coherence estimates are often strong functions of signal to noise ratio and coherent multipath interference [2]. Array gain degradation can result from refractive and scattering effects associated with the ocean surface and water-sediment interface, also from volume, internal wave, and other structural effects. The use of an array of sensors to measure coherence length and array signal gain benefits from having larger degrees of freedom, providing larger signal to noise ratios and filtering of unwanted noise sources. Coherence length estimates can be related to signal gain, provided that other causes of signal degradation can be removed.

The method presented in this discussion is an alternative look at coherence, more directed at characterizing propagating fields. As a function of spatial lag, we compute the zero time lag cross-correlation value for pulsed time series, after accounting for the time shift associated with the non-broadside incidence of the incoming plane wave. Figure 5 shows cross-correlation estimates corresponding to the two times whose acoustic arrivals were observed and synthesized in Figs. 3 and 4, above. During the calm time, the fields have similar coherence scale, somewhat coincidentally, because the match is not perfect.

As expected from visual inspection of the acoustic arrivals, coherence length is much longer during the calm ocean state than during the active.

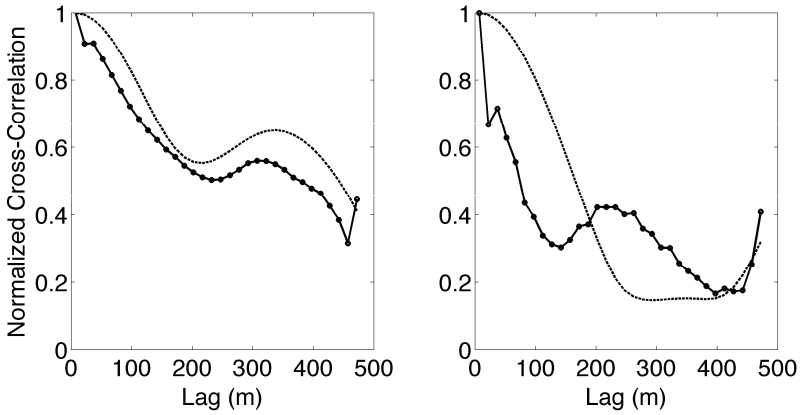

Fig.5: Relative acoustic coherence along the horizontal line array during both times of calm (left) and active (right) ocean state. The measured acoustic field (solid dotted curve) is compared against the synthesized field (dashed curve). Coherence is estimated, as a function of spatial lag, to be the zero time lag cross-correlation value for a pulsed time series.

Table 1 gives temporal and spatial coherence scale estimates during the two times considered in Fig. 5. The coherence scale *D* is defined here to be the point where the coherence function (with units of the square of pressure squared in non-normalized form) falls to one-half. The spatial estimates are taken from the Fig. 5 curves. Multiply by sin(25º) to convert to transverse scale. The temporal scales are extrapolated because the coherence functions do not fall to one-half over the 90-second transmission sequences.

	No Internal Waves		**Internal Waves**	
	D (m)	D / λ	*D (m)*	D / λ
Spatial, Actual	220 *	15	75	5.0
Spatial, Synthesized	240 *	16	160	10
Temporal, Actual	780 s		140 s	

*Table 1: Spatial coherence scale estimates of the measured and synthesized acoustic signals along the horizontal array, and temporal coherence scale measured at one phone. Acoustic wavelength (λ) normalized spatial estimates are also shown. * These values are taken where the curves approach one-half.*

5. CONCLUSIONS

Methods to investigate horizontal coherence using an L-array with non-broadside alignment, of acoustic fields consisting of many normal modes have been examined. A simple method to synthesize horizontal fields using vertical mode decomposition techniques allows simple interference of a homogenous mode structure to be distinguished from decorrelation resulting from azimuthally-varying adiabatic and coupled mode

propagation. Acoustic arrivals during time periods with strong internal waves were observed to cause strong mode coupling effects and to spread mode arrivals. On the contrary, arrivals during a calm period were observed to have clearly separated modal arrivals with little mode multipath effect. Coherence length estimates for broadband pulses during the period of large internal waves are observed to be much shorter than during the period of small internal waves, in line with expectation. An inference is that upper bounds of horizontal coherence scale obtained using a VLA may be close to actual values in some situations, but may be overestimates at other times. The overestimates will occur when mode structure at a receiver has strong azimuthal variability. Finally, many more acoustic arrivals need to be analyzed to obtain meaningful coherence function estimates with good statistical reliability and the effect of noise on the estimates should be examined.

6. ACKNOWLEDGEMENTS

We acknowledge the use of processing codes written by Arthur Newhall and Ying-Tsong Lin. We thank Harry Deferrari and Hien Nguyen for helping with analysis of sounds from the Miami source. The work of many people enabled this large field program. Professor William Carey is thanked for helpful discussions of coherence length.

REFERENCES

[1] **Orr, M. H., B. H. Pasewark, S. N. Wolf, J. F. Lynch, T. Schroeder, and C.-S. Chiu,** South China Sea internal tide/internal waves – Impact on the temporal variability of horizontal array gain at 276 Hz, *IEEE J. Oceanic Eng.,* volume 29, pp. 1292-1307, 2004.

[2] **Carey, W. M.,** The determination of signal coherence length based on signal coherence and gain measurements in deep and shallow water, *J. Acoust. Soc. Am.,* volume 104, pp. 831-837, 1998.

[3] **Duda, T. F.,** Temporal and cross-range coherence of sound travelling through shallow-water nonlinear internal wave packets, *J. Acoust. Soc. Am.,* volume 119, pp. 3717-3725, 2006.

[4] **Finette, S., and R. Oba,** Horizontal array beamforming in an azimuthally anisotropic internal wave field, *J. Acoust. Soc. Am*., volume 114, pp. 131-144, 2003.

[5] **Tollefson, D., M. J. Wilmot and R. Chapman,** Temporal and cross-range coherence of sound travelling through shallow-water nonlinear internal wave packets, *IEEE J. Oceanic Eng.,* volume 30, pp. 764-772, 2005.

[6] **Newhall, A. E., T. F. Duda, K. von der Heydt, J. D. Irish, J. N. Kemp, S. A. Lerner, S. P. Liberatore, Y.-T. Lin, J. F. Lynch, A R. Maffei, A. K. Morozov, A. Shmelev, C, J. Sellers and W. E. Witzell,** Acoustic and oceanographic observations and configuration information for the WHOI moorings from the SW06 experiment, WHOI Technical Report, Woods Hole, MA, 2007

[7] **Headrick, R. H.**, Analysis of Internal Wave Induced Mode Coupling Effects on the 1995 SWARM Experiment Acoustic Transmissions, Ph. D. Thesis, MIT/WHOI, 97-21, 1997.

[8] **Tindle, C. T., K. M. Guthrie, G. E. J. Bold, M. D. Johns, D. Jones, K. O. Dixon, and T. G. Birdsall,** Measurements of the frequency dependence of normal modes*, J. Acoust. Soc. Am.,* volume 64, pp. 1178-1185, 1978.